Advances in Mathematics: Scientific Journal **9** (2020), no.9, 6435–6446
ISSN: 1857-8365 (printed); 1857-8438 (electronic)
https://doi.org/10.37418/amsj.9.9.1

HEAT AND MASS TRANSFER EFFECTS OF CASSON FLUID IN THE ENTRANCE OF CONCENTRIC ANNULI WITH MOVIMENT OF WALLS

SRINIVASA RAO NADIMINTI[1] AND A.KANDASAMY

ABSTRACT. Heat and mass transfer effects of Casson fluid in the entrance of concentric annuli with moviment of inner wall was analyzed here. The problem analysis concerns the simultaneous development of thermal boundary layers and hydrodynamic in concentric walls, one ring is isothermal and the other wall being adiabatic. With the assumption that the inner ring rotates with a fixed angular velocity, also the outer ring is at rest. The finite difference technique is applied to find the velocity Profiles, variation of pressure in the radial coordinate direction and temperature changes in the same direction. Calculation results are obtained for different annular gap values, Casson number and Prandtl's number. The comparison of the results for different special cases was made and observed.

1. INTRODUCTION

Heat and mass transfer effects of Casson fluid in the entrance of concentric annuli with moviment of inner wall having practical importance in technical applications like, axial flow turbo machinery and polymer processing industries. Very often, laminar flow operations provide optimal conditions to maintain a low pumping power proportionally to the heat transfer rate. Also in the field of nuclear reactors, this is happening when the cooling rates reduced. In the event

[1]*corresponding author*

2010 *Mathematics Subject Classification.* 80M20.

Key words and phrases. Entrance Flow, Concentric Annuli, Heat Transfer, Casson Fluid.

of turbulent flow, when the heating begins at the inlet of the conduit, the hydrodynamic boundary layers are generally linear near the inlet of the conduit and the turbulence transitions occur at a distance downstream of the inlet. Therefore, it is necessary to take into account the presence of such a laminar inlet flow in the calculation of heat transfer parameters for a conduit in which the fully developed flow is turbulent. The fluid considered here is the blood model Casson fluid, which belongs to the fluid class with "flow stress independent of time". The Newtonian fluid flow in the entrance region heat transfer problem in a concentric annuli was studied by [4]. [2] developed the stress-strain relation for the Casson fluid with the inner cylinder is at rest and outer cylinder rotating between two rotating cylinders in the annular space. [8] applied finite difference method for the Power-law fluid in the annuli and found difference in the entrance geometries. [12] have applied finite difference technique to analyze the laminar flow of a Power-Law fluid in a concentric annuli with inner wall rotating. [9] studied the flow of the Bingham plastic fluids in the concentric annulus and analyzed the results for centre core velocity, pressure drop and boundary layer thickness. [6] given the Casson fluid constitutive equation

$$\tau^{\frac{1}{2}} = {\tau_0}^{\frac{1}{2}} + K_c \dot{\gamma}^{\frac{1}{2}}$$

The fluid shear stress is denoted by τ. $\dot{\gamma}$ is represented the strain rate. τ_0, K_c^2 are the yield value and Casson's viscosity.

Further, Flow of Casson fluid in a pipe filled with a homogeneous porous medium has been considered by [5]. [1] investigated Magneto hydrodynamic flow of a non-Newtonian fluid in an eccentric annulus with heat transfer. Analytical solution in the entrance region blood flow in a concentric annuli has been obtained by [3] assuming the blood to obey Casson model. Recently, [7,11] investigated the flow of Herschel-Bulkley and Bingham fluids in the entrance region of concentric annuli with the inner wall rotation. Casson fluid flow with a side branch in a narrow tube has been investigated by [10]. The problem of Heat and mass transfer effects of Casson fluid in the entrance of concentric annuli with moviment of inner wall was analyzed here.

2. Problem Formulation

The Casson fluid entered in to the concentric rings horizontally with R_1 and R_2 are the inner and outer radius respectively, with the uniform velocity u_0 along the axial direction with p_0 as the initial pressure and t_0 as the initial temperature. The non-rotating outer ring is at rest and the inner ring rotating with the angular velocity ω. The flow is incompressible, laminar, axisymmetric with constant physical properties, with no internal heat generation and negligible viscous dissipation. Figure 1 shows the geometry of the problem. Equations in cylindrical polar coordinates apted to the geometry of the problem for the Casson fluid are

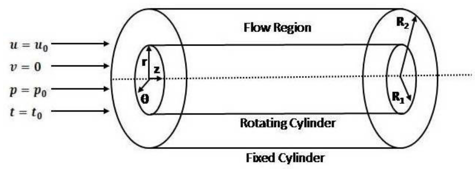

FIGURE 1. Geometry of the Problem

(2.1) Equation of Continuity : $\dfrac{\partial(rv)}{\partial r} + \dfrac{\partial(ru)}{\partial z} = 0$

$$\theta - \text{mom. eqn.} : v\frac{\partial w}{\partial r} + u\frac{\partial w}{\partial z} + \frac{vw}{r} = \frac{1}{\rho r^2}\frac{\partial}{\partial r}\left(r^2\left(\tau_0 + K_c^2 r\frac{\partial}{\partial r}(\frac{w}{r}) + 2K_c\sqrt{\tau_0 r\frac{\partial}{\partial r}(\frac{w}{r})}\right)\right)$$

(2.2) r – momentum equation : $\dfrac{w^2}{r} = \dfrac{1}{\rho}\dfrac{\partial p}{\partial r}$

$$z - \text{mom. eqn.} : v\frac{\partial u}{\partial r} + u\frac{\partial u}{\partial z} = -\frac{1}{\rho}\frac{\partial p}{\partial z} + \frac{1}{\rho r}\frac{\partial}{\partial r}\left(r\left(\tau_0 + K_c^2\frac{\partial u}{\partial r} + 2K_c\sqrt{\tau_0\frac{\partial u}{\partial r}}\right)\right)$$

(2.3) Energy equation : $v\dfrac{\partial t}{\partial r} + u\dfrac{\partial t}{\partial z} = \alpha\left[\dfrac{\partial^2 t}{\partial r^2} + \dfrac{1}{r}\dfrac{\partial t}{\partial r}\right]$

Here the velocities in the direction z, r, θ represented by u,v,w, temperature of the fluid is denoted by t, ρ is the fluid density, pressure of the fluid is denoted by p and α represent the thermal diffusivity. Following are the hydrodynamic part boundary conditions

$$\begin{aligned} \text{at } z &= 0, p = p_0 \\ \text{at } z &= 0\ , R_1 < r < R_2, u = u_0 \\ \text{with } z &\geq 0\ , r = R_1, v = u = 0 \text{ and } w = \omega R_1 \\ \text{with } z &\geq 0\ , r = R_2, v = u = w = 0 \end{aligned} \tag{2.4}$$

Continuity equation (2.1) with the boundary conditions (2.4) can be expressed as:

$$\int_{R_1}^{R_2} 2rudr = (R_2^2 - R_1^2)u_0 \tag{2.5}$$

$$\begin{aligned} R &= \frac{r}{R_2}, U = \frac{u}{u_0}, V = \frac{\rho v R_2}{K_c^2}, W = \frac{w}{\omega R_1}, N = \frac{R_1}{R_2}, P = \frac{p - p_0}{\rho u_0^2}, Z = \frac{2z(1-N)}{R_2 Re} \\ T &= \frac{t - t_0}{t_w - t_0}, Y_c = \frac{\tau_0 R_2}{u_0 K_c^2}, Re = \frac{2R_2(1-N)\rho u_0}{K_c^2}, Pr = \frac{\mu C_p}{K}\left(\frac{R_2}{u_0}\right)^{\frac{1}{2}}, \end{aligned}$$

where Y_c is the Casson number, T_a Taylors number, Re Reynolds number, μ_r is the viscosity, K is the thermal conductivity, C_p denotes the specific heat at constant temperature, Pr denotes the Prandtl's number and N is the annular gap of the annuli. Dimensionless equations of (2.1)-(2.3) and (2.5) are the following

$$\begin{aligned} \frac{\partial V}{\partial R} + \frac{V}{R} + \frac{\partial U}{\partial Z} &= 0 \\ V\frac{\partial W}{\partial R} + U\frac{\partial W}{\partial Z} + \frac{VW}{R} &= \frac{4Y_c^{\frac{1}{2}}}{R}\left(\frac{\partial W}{\partial R} - \frac{W}{R}\right)^{\frac{1}{2}} + Y_c^{\frac{1}{2}}\left(\frac{\partial W}{\partial R} - \frac{W}{R}\right)^{-\frac{1}{2}} * \\ &\quad \left(\frac{\partial^2 W}{\partial R^2} - \frac{1}{R}\frac{\partial W}{\partial R} + \frac{W}{R^2}\right) + \left(\frac{\partial^2 W}{\partial R^2} + \frac{1}{R}\frac{\partial W}{\partial R} - \frac{W}{R^2}\right) + \frac{2Y_c}{R} \\ \frac{W^2}{R} &= \frac{Re^2(1-N)}{2(1+N)T_a}\frac{\partial P}{\partial R} \\ V\frac{\partial U}{\partial R} + U\frac{\partial U}{\partial Z} &= -\frac{\partial P}{\partial Z} + \frac{1}{R}\frac{\partial U}{\partial R} + \frac{2Y_c^{\frac{1}{2}}}{R}\left(\frac{\partial U}{\partial R}\right)^{\frac{1}{2}} + \\ &\quad Y_c^{\frac{1}{2}}\left(\frac{\partial U}{\partial R}\right)^{-\frac{1}{2}}\frac{\partial^2 U}{\partial R^2} + \frac{\partial^2 U}{\partial R^2} + \frac{Y_c}{R} \end{aligned}$$

(2.6) $$V\frac{\partial T}{\partial R} + U\frac{\partial T}{\partial Z} = \frac{1}{Pr}\left[\frac{\partial^2 T}{\partial R^2} + \frac{1}{R}\frac{\partial T}{\partial R}\right],$$

also

(2.7) $$\int_N^1 2RUdR = (1 - N^2).$$

The dimensionless boundary conditions for the hydrodynamic part associated with the boundary conditions (2.4) are given by

(2.8) $$\begin{aligned} \text{at } Z &= 0\,,\, N < R < 1, U = 1 \\ \text{at } Z &= 0, P = 0 \\ \text{with } Z &\geq 0\,,\, R = 1, V = U = W = 0 \\ \text{with } Z &\geq 0\,,\, R = N, V = U = 0\,,\, W = 1\,. \end{aligned}$$

For the thermal problem, we solved the problem with the following boundary conditions, considering the non-rotating ring to be adiabatic and the rotating ring to be isothermal are given by

(2.9) $$\begin{aligned} \text{at } Z &= 0\,,\, N < R < 1, T = 0 \\ \text{with } Z &\geq 0, \frac{\partial T}{\partial R} = 0\,,\, R = 1 \\ \text{with } Z &\geq 0, T = 1\,,\, R = N\,. \end{aligned}$$

3. NUMERICAL SOLUTION

Figure 2 show the mesh network for the given problem and the following difference representations are taken. We adopted and considered the numerical method from the work of [4]. The radial and axial direction grid sizes are represented by ΔR and ΔZ respectively.

(3.1) $$\frac{W^2_{i,j+1}}{N + i\Delta R} = \frac{(1-N)Re^2}{2T_a(1+N)}\frac{P_{i,j+1} - P_{i-1,j+1}}{\Delta R}$$

(3.2) $$V_{i+1,j+1} = V_{i,j+1}\left(\frac{N + i\Delta R}{N + (i+1)\Delta R}\right) - \frac{\Delta R}{4\Delta Z}\left(\frac{2N + (2i+1)\Delta R}{N + (i+1)\Delta R}\right) * (U_{i+1,j+1} + U_{i,j+1} - U_{i+1,j} - U_{i,j})$$

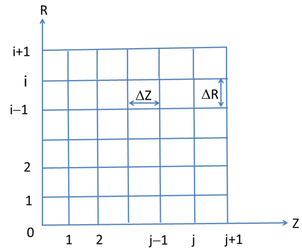

FIGURE 2. Grid Representation for the Problem

$$P_{i,j+1} + U_{i-1,j+1} * \left[\frac{\Delta Z}{2\Delta R(N+i\Delta R)} - \frac{\Delta Z}{2\Delta R}V_{i,j} - \frac{\Delta Z}{(\Delta R)^2} - \frac{(Y_c)^{1/2}\Delta Z}{(\Delta R)^2}\left(\frac{U_{i+1,j+1}-U_{i-1,j+1}}{2(\Delta R)}\right)^{-1/2}\right] + U_{i,j+1}\left[U_{i,j} + \frac{2\Delta Z}{(\Delta R)^2} + \frac{2(Y_c)^{1/2}\Delta Z}{(\Delta R)^2}\left(\frac{U_{i+1,j+1}-U_{i-1,j+1}}{2(\Delta R)}\right)^{-1/2}\right] + U_{i+1,j+1} * \left[-\frac{\Delta Z}{2\Delta R(N+i\Delta R)} + \frac{\Delta Z}{2\Delta R}V_{i,j} - \frac{\Delta Z}{(\Delta R)^2} - \frac{(Y_c)^{1/2}\Delta Z}{(\Delta R)^2}\left(\frac{U_{i+1,j+1}-U_{i-1,j+1}}{2(\Delta R)}\right)^{-1/2}\right] - \frac{2(Y_c)^{1/2}\Delta Z}{N+i\Delta R}\left(\frac{U_{i+1,j+1}-U_{i-1,j+1}}{2(\Delta R)}\right)^{1/2} = P_{i,j} + U_{i,j}^2 + \frac{Y_c(\Delta Z)}{N+i\Delta R} \quad (3.3)$$

$$Vi,j\left[\frac{W_{i+1,j+1}+W_{i+1,j}-W_{i-1,j}-W_{i-1,j+1}}{4\Delta R}\right] + Ui,j\left[\frac{W_{i,j+1}-W_{i,j}}{\Delta Z}\right] + \frac{V_{i,j}W_{i,j}}{N+i\Delta R} = \frac{4(Y_c)^{1/2}}{N+i\Delta R}\left[\frac{W_{i+1,j+1}+W_{i+1,j}-W_{i-1,j}-W_{i-1,j+1}}{4\Delta R} - \frac{W_{i,j}}{N+i\Delta R}\right]^{\frac{1}{2}} + (Y_c)^{1/2}\left[\frac{W_{i+1,j+1}+W_{i+1,j}-W_{i-1,j}-W_{i-1,j+1}}{4\Delta R} - \frac{W_{i,j}}{N+i\Delta R}\right]^{-\frac{1}{2}} * \left(\frac{W_{i+1,j+1}+W_{i+1,j}-2W_{i,j+1}-2W_{i,j}+W_{i-1,j}+W_{i-1,j+1}}{2(\Delta R)^2} - \frac{W_{i+1,j+1}+W_{i+1,j}-W_{i-1,j}-W_{i-1,j+1}}{(N+i\Delta R)4\Delta R} + \frac{W_{i,j}}{(N+i\Delta R)^2}\right)$$

$$+(\frac{W_{i+1,j+1}+W_{i+1,j}-2W_{i,j+1}-2W_{i,j}+W_{i-1,j}+W_{i-1,j+1}}{2(\Delta R)^2}+ \frac{W_{i+1,j+1}+W_{i+1,j}-W_{i-1,j}-W_{i-1,j+1}}{(N+i\Delta R)4\Delta R}-\frac{W_{i,j}}{(N+i\Delta R)^2})+\frac{2Y_c}{N+i\Delta R} \tag{3.4}$$

Here R=N at i=0 and R=1 at i=m. equation (2.7) with the trapezoidal rule application gives

$$\frac{\Delta R}{2}(NU_{0,j}+U_{m,j})+\Delta R\sum_{i=1}^{m-1}U_{i,j}(N+i\Delta R)=\left(\frac{1-N^2}{2}\right). \tag{3.5}$$

The above equation converts to with the boundary condition (2.8).

These group of equations (3.1)-(3.5) are solved by the iterative procedure, using Newton-Raphson technique upto the flow becomes developed fully in the both axial and tangential directions.

Using the known velocity profiles U and V, the equation of energy (2.6), solved as a linear equation in T. The energy equation with the implicit finite difference method represented by

$$\begin{aligned}
&Ti-1,j+1\left[\frac{1}{4(N+i\Delta R)Pr\Delta R}-\frac{V_{i,j+1}+V_{i,j}}{8\Delta R}-\frac{1}{2Pr(\Delta R)^2}\right]+\\
&Ti+1,j+1\left[\frac{V_{i,j+1}+V_{i,j}}{8\Delta R}-\frac{1}{2Pr(\Delta R)^2}-\frac{1}{4(N+i\Delta R)Pr\Delta R}\right]+\\
&Ti,j+1\left[\frac{U_{i,j+1}+U_{i,j}}{2\Delta Z}+\frac{1}{Pr(\Delta R)^2}\right]=\\
&Ti+1,j\left[\frac{1}{2Pr(\Delta R)^2}+\frac{1}{4(N+i\Delta R)Pr\Delta R}-\frac{V_{i,j+1}+V_{i,j}}{8\Delta R}\right]+\\
&Ti-1,j\left[\frac{V_{i,j+1}+V_{i,j}}{8\Delta R}-\frac{1}{2Pr(\Delta R)^2}-\frac{1}{4(N+i\Delta R)Pr\Delta R}\right]+\\
&Ti,j\left[\frac{U_{i,j+1}+U_{i,j}}{2\Delta Z}-\frac{1}{Pr(\Delta R)^2}\right].
\end{aligned} \tag{3.6}$$

To get the temperature profiles of the problem, the equation (3.6) have been solved along with boundary conditions (2.9).

4. Analysis and Conclusion

The finite difference analysis have been obtained for different numbers of Casson Number Y_c, annular gap values N and various parameters as shown in

Table 1. Number 15 chosen as the Prandtl's number. Here, the velocity profiles, temperature and pressure of the annuli have been shown in following figures.

Also we have choosen Aspect ratio as 0.3, 0.8 and the corresponding Radial Position as 0.1, 0.05, Axial Position as 0.01, 0.03.

Figures 3 to 4 show the velocity profiles in the tangential direction with aspect ration values 0.8 and 0.3 and for different values of Casson numbers Y_c with Prandtl's number 15. The computation has been done for various values of the parameter Rt to study the effect of rotation of inner cylinder. The values corresponding to $Rt=1$ and 20 are depicted in the figures. The tangential velocity values are low from the inner ring to the non-rotating outer ring of the annuli. Also it is observed that with the high of annular gap N, the tangential velocity profiles are also high. Further, as observed for the other yield-stress fluid, viz. Bingham fluid, also it is observed that with the increment of Casson value(number), the tangential velocity profiles are increasing.

Figures 5 to 6 show the velocity profiles in the axial direction with aspect ration values 0.8 and 0.3 at axial positions of Z = 0.01, 0.03 and for various values of the Casson numbers Y_c. Also observed that, with increment of the aspect ratio N, the axial velocities are high at all values of Casson numbers Y_c. Then it is found, the velocity profile looks the parabolic shape with Casson number Y_c being zero (Newtonian fluid).

The velocity profiles along the radial direction with aspect ration values 0.8 and 0.3 for various values of the Casson numbers Y_c at different axial positions Z are shown in Figures 7 to 8. Again, the parameter Rt values are taken as 1 and 20 for computational purpose. At the region near the non-rotating outer ring the radial velocity values are negative, because it is in the radial coordinate opposite direction. Near the rotating inner ring, it has the positive values since it is in same radial coordinate direction. The values of the radial velocity decreases with increase of Casson number Y_c. Because of the angular rotation of the inner ring of the annulus this phenomena is observed.

Figures 9 to 10 show the pressure variation in the radial direction R with aspect ration values 0.8 and 0.3 for different values of Casson numbers Y_c. It is observed that the values of P increases from the low at the rotating ring to a high at the non-rotating outer ring of the annulus. Also, it is observed that increment in the value of Casson numbers Y_c, decrease the pressure values P.

Further, it is noted that near the outer wall region the pressure is not changed much when compare with the radial direction.

Figures 11 to 18 show the distribution of temperature T for N=0.3, 0.8 at axial positions of Z=0.02, 0.03, 0.04, 0.05 and Z=0.01, 0.02, 0.03, 0.04 for various values of Casson number Y_c=0, 10, 20, 30. Here the Prandtl's number is fixed as 15. Also it is noted with the previous observations, the distribution of temperature is low with the high Casson Numbers for a fixed annular gap. With the annular gap *N* is high, the temperature is also high for a constant Casson Number value. then, noted that with the high axial direction values the temperature is high for a constant annular gap *N* and Casson Number Y_c. The present results are compared with other recent work done for a particular case of stationary cylinders

Here we presented the numerical solution to the blood model casson fluid in entrance zone of concentric annuli. The aspect ratio number N, Prandtl's and Casson number effects on the distribution of temperature are analyzed. The results were estimated for all the values of the Casson number, Prandtl's number and the aspect ratio N. The distribution of the temperature in the radial coordinate direction has been geometrically represented and the comparison of the current results with the available results in literature for different special cases was made and observed to be concordant.

From the above analysis, the following points can be drawn:

(1) From the above figures we can say that, from the inner ring to the non-rotating outer ring of the annuli, the tangential profiles are decreases.
(2) With a fixed Casson number Y_c, the velocity *U* increases along the axial direction, if we decrease the annular gap.
(3) The pressure is found to be low at the rotating wall and gradually increasing to a high at the non-rotating wall for all values of Casson numbers Y_c. and pressure variation is not much considered along the radial direction near the non-rotating wall of the annulus.
(4) As observed in the case of Bingham study here also the temperature decreases from the inner ring to the non-rotating outer ring.
(5) Temperature is decreasing when we increase the Casson number Y_c and the same phenomena is observed for the increment of aspect ratio *N*.

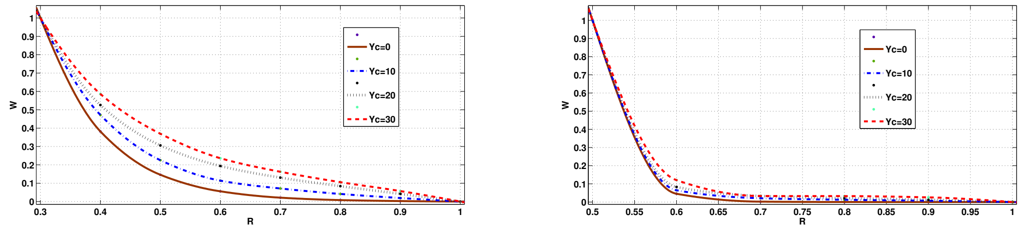

FIGURE 3. Tangential Velocity Profiles for different annular Gaps

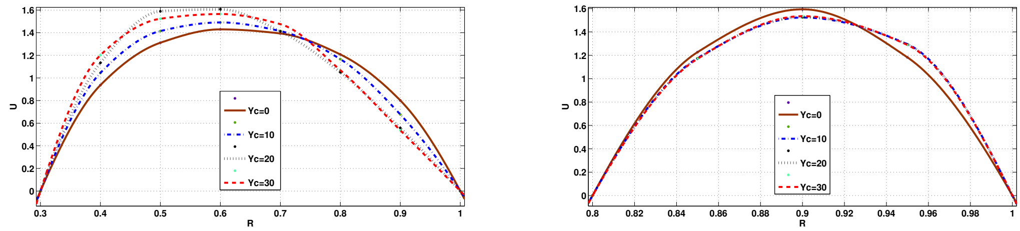

FIGURE 4. Axial Velocity Profiles for different annular Gaps

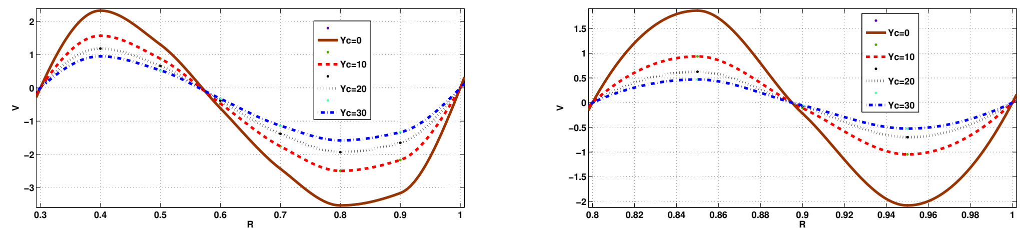

FIGURE 5. Radial Velocity Profiles for different annular Gaps

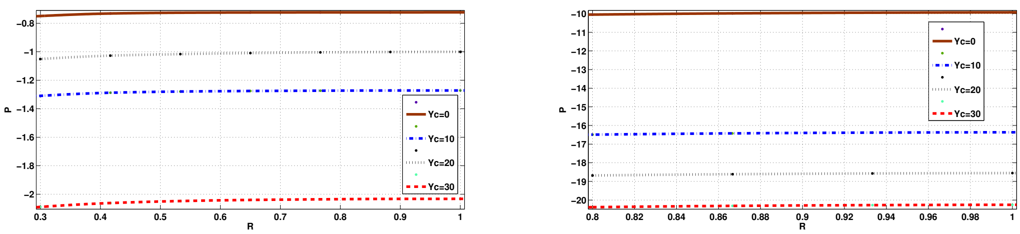

FIGURE 6. Pressure Variation for different annular Gaps

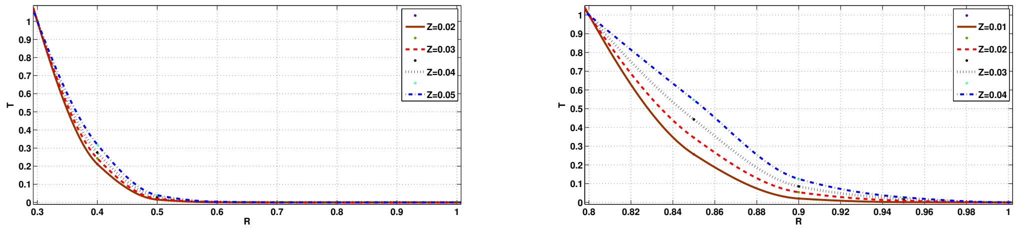

FIGURE 7. Temperature Profiles for different annular Gaps

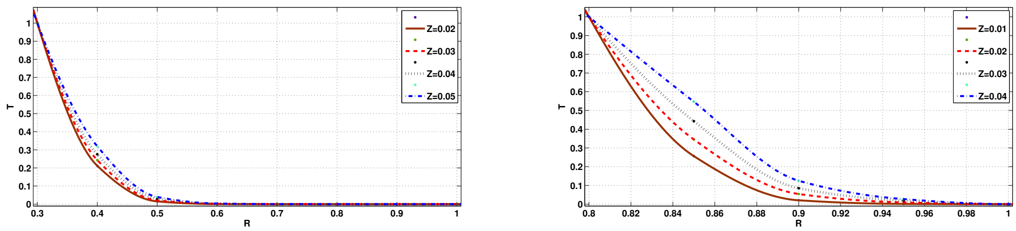

FIGURE 8. Temperature Profiles for different annular Gaps

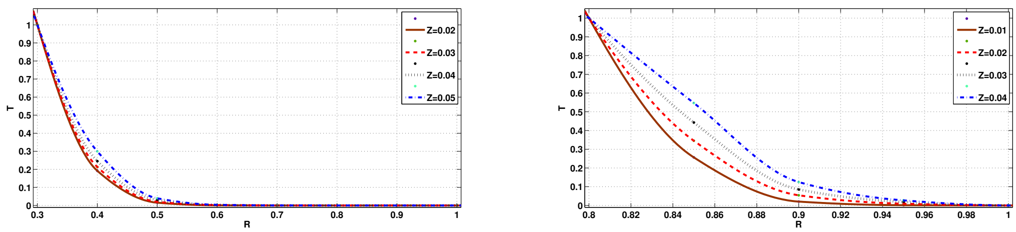

FIGURE 9. Temperature Profiles for different annular Gaps

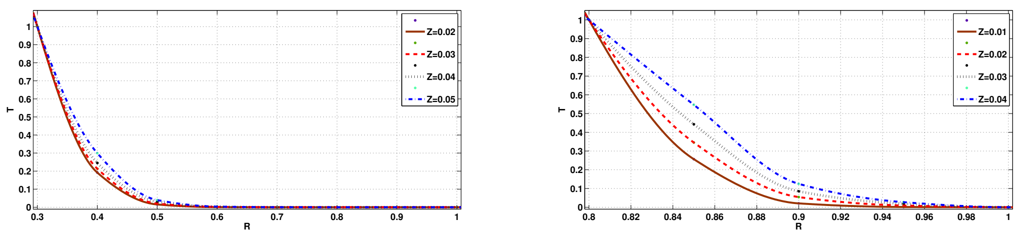

FIGURE 10. Temperature Profiles for different annular Gaps

REFERENCES

[1] M. E. S. AHMED, H. A. ATTIA: *Magneto hydrodynamic flow and heat transfer of non-Newtonian fluid in an eccentric annulus*, Canadian Journal of Physics, **76** (1998), 391–401.

[2] R. L. BATRA, B. DAS: *Flow of a Casson Fluid between Two Rotating Cylinders*, Fluid Dynamic Research, **9** (1992), 133–141.

[3] R. L. BATRA, B. JENA: *Entrance region flow of blood in concentric annulus*, International Journal of Engineering Science, **28** (1990), 407–419.

[4] J. E. R. CONEY, M. A. I. EL-SHAARAWI: *A contribution to the numerical solution of developing laminar flow in the entrance region of concentric annuli with rotating inner walls*, ASME Trans. Journal of Fluid Engineering, **96** (1974), 333–340.

[5] R. K. DASH, K. N. MEHTA, G. JAYARAM: *Casson fluid flow in a pipe filled with a homogeneous porous medium*, International Journal of Engineering Science, **34** (1996), 1145–1156.

[6] Y. C. FUNG: *Biomechanics: Mechanical Properties of Living Tissues* New York: Springer, 1981.

[7] A. KANDASAMY, S. RAO NADIMINTI: *Entrance region flow in concentric annuli with rotating inner wall for Herschel-Bulkley fluids*, International Journal of Applied and Computational Mathematics, **1**(2) (2015), 235–249.

[8] M. C. A. MAIA, C. A. GASPARETTO: *A numerical solution for entrance region of non-Newtonian flow in annuli*, Brazilian Journal of Chemical Engineering, **20** (2003), 201–211.

[9] I. M. MISHRA, S. KUMAR: *Entrance Region Flow of Bingham Plastic Fluids in Concentric Annulus*, Indian Journal of Technology, **23** (1985), 81–87.

[10] J. C. MISRA, S. K. GHOSH: *Flow of a Casson fluid in a narrow tube with a side branch*, International Journal of Engineering science, **38** (2000), 2045–2077.

[11] A. KANDASAMY, S. R. NADIMINTI: *Entrance region flow in concentric annuli with rotating inner wall for Bingam fluids*, Journal of Computational and Applied Mechanics, **11**(2) (2016), 137–157.

[12] M. E. SAYED-AHMED, H. SHARAF-EL-DIN: *Entrance region flow of a power-law fluid in concentric annuli with rotating inner wall*, International Communications in Heat and Mass Transfer, **33** (2006), 654–665.

DIVISION OF MATHEMATICS, DEPARTMENT OF SCIENCE AND HUMANITIES
VIGNAN'S FOUNDATION FOR SCIENCE, TECHNOLOGY AND RESEARCH (VFSTR)
VADLAMUDI, GUNTUR, ANDHRAPRADESH - 522213, INDIA
E-mail address: srinudm@gmail.com

DEPARTMENT OF MATHEMATICAL AND COMPUTATIONAL SCIENCES
NATIONAL INSTITUTE OF TECHNOLOGY KARNATAKA, SURATHKAL
MANGALORE, KARNATAKA-575025, INDIA
E-mail address: kandy@nitk.ac.in